

SUPPLEMENTAL MATERIAL

- **SUPPLEMENTAL METHODS**
- **SUPPLEMENTAL TABLES**
 - Supplemental Table S1
 - Supplemental Table S2
 - Supplemental Table S3
- **SUPPLEMENTAL FIGURES**
 - Supplemental Figure S1
 - Supplemental Figure S2
- **SUPPLEMENTAL REFERENCES**
- **SUPPLEMENTAL VIDEO LEGENDS**
 - Video Legend 1A-D.
 - Video Legend 2A-D.
 - Video Legend 3A-E.
 - Video Legend 4A-E.
 - Video Legend 5A-C.

SUPPLEMENTAL METHODS

Ultrasound Imaging and Doppler Echocardiography

When fetal ultrasound was performed, the mother's bladder was used as an anatomic landmark to locate fetuses proximally from the cervix to more distally in the uterine horn on the left as L1,2,3, etc., and on the right as R1,2,3, etc. The imaging modalities used included B-mode imaging, and color flow and spectral Doppler, and M-mode imaging as previously described^{1,2}. The initial Acuson scan was used to determinate litter size, orientation of fetuses and developmental staging of the fetuses with crown to rump length and fetus area measurements. Crown-to-rump length of fetus > two standard deviations below the mean compared to age-matched normal fetuses were considered growth restricted³.

Analysis of Positive and Negative Predictive Value with Vevo2100 Ultrasound Imaging

Fetuses examined by the Acuson-Vevo2100 two-tier ultrasound screen were subsequently analyzed by EFIC histology as the gold standard for CHD diagnosis. This included fetuses that were Vevo ultrasound diagnosed with CHD, fetuses Vevo ultrasound diagnosed as without CHD from the same litters with fetuses Vevo diagnosed with CHD, and fetuses from entire litters that were Vevo ultrasound diagnosed as without CHD. Provisional CHD diagnoses were made based on the ultrasound findings. Then after the EFIC imaging data was obtained, a panel of pediatric cardiologists and a pediatric pathologist reviewed the data and made consensus CHD diagnoses. The CHD diagnosis determined by EFIC imaging was compared to the diagnosis made by Vevo ultrasound imaging to determine the number of true positives, false positives, true negatives and false negatives. Using these numbers, the positive predictive value (PPV) and negative predictive value (NPV) were calculated. The

PPV = (number of true positives) / (number of true positives + number of false positives); the

NPV = (number of true negatives) / (number of true negatives + number of false negatives).

SUPPLEMENTAL TABLES

Table S1. Developmental anomalies detected by fetal ultrasound

Defects	Pedigrees*	G2 Females [†]	Total Fetuses [‡]	Abnormal Fetuses [§]	Cardiac Defects	%Abnormal Fetus/Litter [#]
Total Screened	1,381	5,745	46,270	2,590		
Cardiac Anomalies	664 (48.1%)	1,095 (19.1%)	1,722 (3.7%)	66.5%		20.9%
Prenatal Lethality	523 (37.9%)	871 (15.2%)	1,189 (2.6%)	45.9%	481 (40.5%)	20.0%
Growth Retarded	130 (9.4%)	168 (2.9%)	204 (0.4%)	7.9%	181 (88.7%)	17.7%
Hydrops	303 (21.9%)	425 (7.4%)	635 (1.4%)	24.5%	271 (42.7%)	20.8%
Craniofacial/Limb Defects	109 (7.9%)	143 (2.5%)	221 (0.5%)	8.5%	143 (64.7%)	20.6%
Body Wall Defects	34 (2.5%)	41 (0.7%)	61 (0.1%)	2.4%	49 (80.3%)	22.1%
Heterotaxy/ Situs Defects	30 (2.2%)	41 (0.7%)	52 (0.1%)	2.0%	48 (92.3%)	19.5%

*Number G1 pedigrees screened. Number in parentheses represents percent pedigrees with indicated defects in total pedigrees screened.

[†]Number G2 females scanned with fetuses exhibiting the indicated defects. Number in parentheses represents percent G2 females with indicated defects in total G2 females screened.

[‡]Number in parentheses represents percent of fetuses with indicated defects in total fetuses screened.

[§]Percent of abnormal fetuses with the indicated defects.

^{||}Fetuses with indicated developmental anomaly in conjunction with cardiac defects. Percent = fetuses with indicated anomaly with cardiac defects/total fetuses with indicated anomaly.

[#]Percent of fetuses with indicated defects amongst all fetuses in the affected litters.

Table S2. Congenital Heart Disease Mutant Lines Archived*

Congenital Heart Defect Phenotype	No. Lines[†]
Lines with CHD	90
Laterality Defects	49
Septal Defects	
Ventricular Septal Defect	64
Atrial Septal Defect	30
Atrioventricular Septal Defect	35
Outflow Tract Malalignments	
Double Outlet Right Ventricle	41
Persistent Truncus Arteriosus/Pulmonary atresia	16
Transposition of Great Arteries	10
Aortic Stenosis/Coarctation	10
Pulmonary Stenosis	16
Tricuspid Atresia	6
Hypoplastic Left Heart Syndrome	3
Hypoplastic Right Heart Syndrome	4
Arch Anomaly	
Right aortic arch	22
Interrupted Aortic Arch	8
Vascular Ring	3
Coronary Fistula	5

*All mutant lines curated in the Mouse Genome Informatics Database (www.informatics.jax.org) and with sperm cryopreserved at the Jackson Laboratory.

[†]Mutant lines may be represented in multiple CHD categories.

Table S3. Accuracy of Vevo2100 Ultrasound Diagnosis of Congenital Heart Disease *

CHD diagnosis	Values Obtained Without the Additional 86 Normal Fetuses		Values Obtained With the Additional 86 Normal Fetuses	
	PPV	NPV	PPV	NPV
Septal Defects†	95.7%	75.6%	95.7%	80.9%
Outflow Tract Defects‡	85.4%	92.1%	85.4%	93.8%
HLHS	100%	100%	100%	100%
HRHS	77.8%	99.5%	77.8%	99.6%
MS/MA	75%	99.5%	75%	99.6%
AS/AA/COA	60%	95.3%	60%	96.1%
Tricuspid Hypoplasia/Atresia	60%	99.1%	60%	99.2%
Pulmonary Stenosis	90%	96.5%	90%	97.1%
Coronary Artery Fistula	71.4%	97.9%	71.4%	98.3%
Cardiac Situs Defects	100%	99%	100%	99%

* Grey columns: Total number fetuses/pups analyzed =438. It included 277 identified with CHD+161 littermates of affected fetuses but ultrasound identified as without CHD.

Clear columns: Total number fetuses/pups analyzed =524. It included 277 identified with CHD+161 littermates of affected fetuses but ultrasound identified as without CHD +86 fetuses from litters that were ultrasound identified as without CHD.

SUPPLEMENTAL FIGURES

Figure S1 Summary of Ultrasound Screen

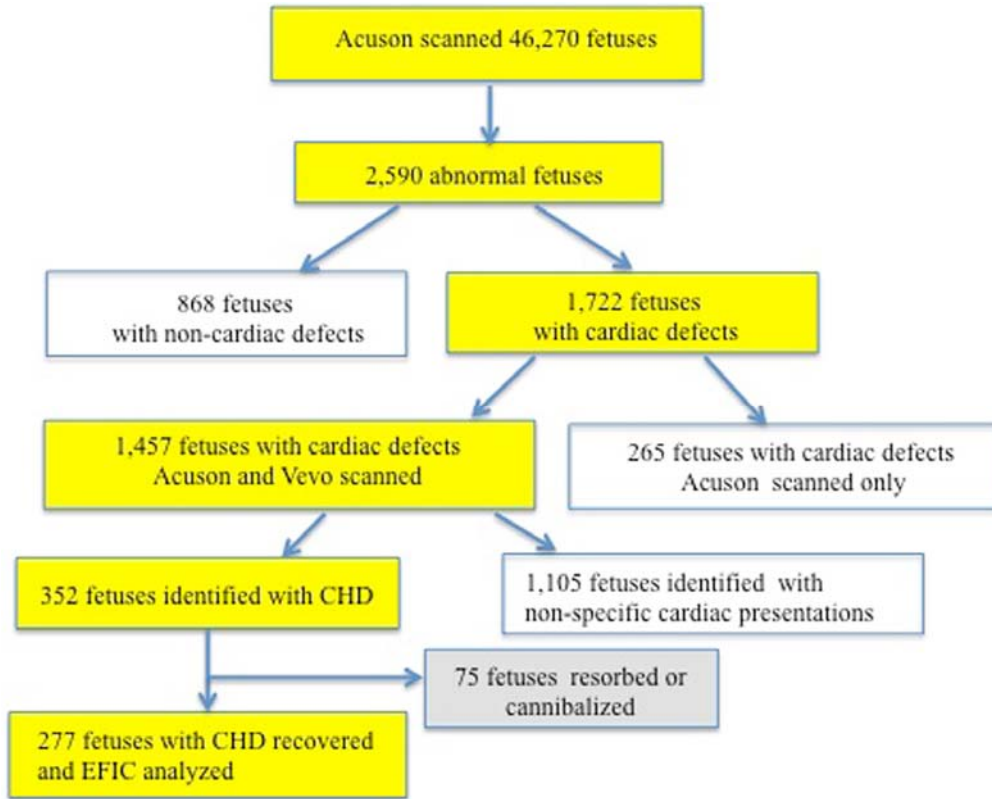
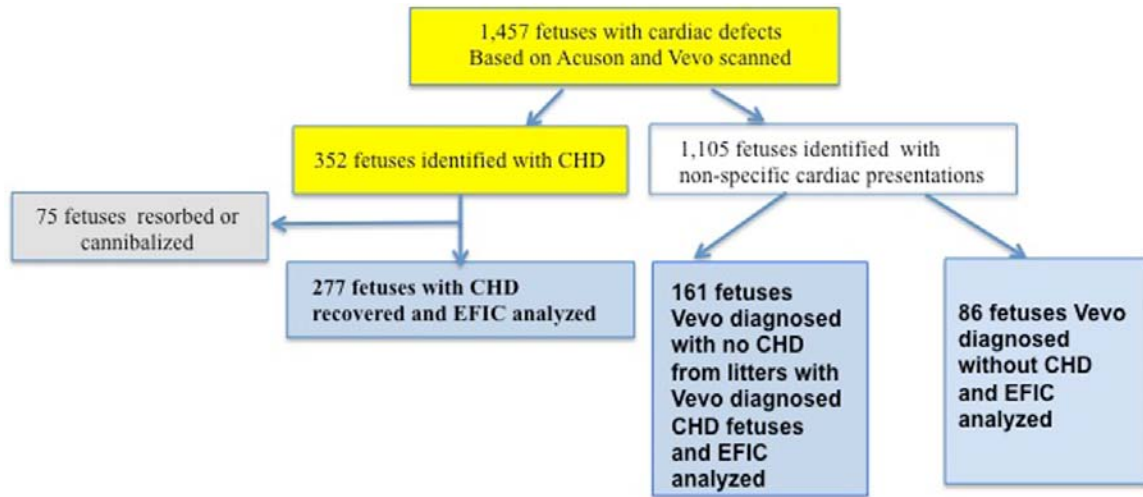


Figure S2. EFIC Imaging Analysis to Assess Accuracy of Vevo2100 Diagnosis of CHD



Note fetuses analyzed by EFIC imaging for CHD confirmation are denoted in the blue boxes.

SUPPLEMENTAL REFERENCES

1. Shen Y, Leatherbury L, Rosenthal J, Yu Q, Pappas MA, Wessels A, Lucas J, Siegfried B, Chatterjee B, Svenson K, Lo CW. Cardiovascular phenotyping of fetal mice by noninvasive high-frequency ultrasound facilitates recovery of ENU-induced mutations causing congenital cardiac and extracardiac defects. *Physiol Genomics*. 2005;24:23-36.
2. Yu Q, Shen Y, Chatterjee B, Siegfried BH, Leatherbury L, Rosenthal J, Lucas JF, Wessels A, Spurney CF, Wu YJ, Kirby ML, Svenson K, Lo CW. ENU induced mutations causing congenital cardiovascular anomalies. *Development*. 2004;131:6211-6223.
3. Yu Q, Leatherbury L, Tian X, Lo CW. Cardiovascular assessment of fetal mice by in utero echocardiography. *Ultrasound Med Biol*. 2008;34:741-752.

VIDEO LEGENDS

VIDEO 1

Video 1A: A fetus was found with hydrops at E13.5 by the Acuson

Video 1B: Hydrops (Arrow) and pericardial effusion (labeled PE with arrow) were detected by further UBM scanning. (PE=pericardial effusion)

Video 1C: The UBM color flow mapping in transverse view showed bidirectional shunt and regurgitation of AVSD.

Video 1D: Acuson scan of the same fetus one day later (E14.5) showed the affected fetus had died, as it exhibited no heart beating.

VIDEO 2

Video 2A: The Acuson imaging in sagittal view detected abnormal blood flow (blue color flow) during diastole.

Video 2B: The UBM 2D imaging in frontal view revealed a gap or hole (labeled CF with arrow) in the ventricular septum. (CF=coronary artery fistula).

Video 2C: UBM color flow mapping in frontal view detected an abnormal vessel (blue flow stream) during diastole (arrow), which originated from the root of the aorta and exited into the RV, suggesting it is a coronary artery fistula.

Video 2D: Micro-MRI confirmed UBM diagnosis of coronary artery fistula.

VIDEO 3

Video 3A: Levocardia as seen in the transverses view by 2D imaging with the Vevo2100.

Video 3B: Right-sided stomach seen in the transverse view by 2D imaging with the Vevo2100.

Video 3C: Vevo2100 color flow mapping in the sagittal view revealed anterior positioning of the aorta, posterior pulmonary artery, and outflow regurgitation, which together indicated transposition of the great arteries.

Video 3D: Vevo2100 color flow mapping in the sagittal view showed two overlapping red flow streams representing anterior aorta with aortic regurgitation, posterior pulmonary artery emerging from the RV, and a subpulmonary VSD. Together these presentations would suggest DORV of the Taussig-Bing type.

Video 3E: EFIC 2D serial image stack of the same fetus confirmed DORV of the Taussig-Bing type.

VIDEO 4

Video 4A: 2D imaging in the transverse view with the Vevo2100 showed atrioventricular septal defect. (CV= common atrioventricular valve)

Video 4B: Color flow mapping using the Vevo2100 showed atrioventricular septal defect with regurgitation in the transverse view.

Video 4C: Pulmonary artery and majority of aorta emerge from the RV with hypoplastic PA seen by UBM 2D imaging in sagittal view.

Video 4D: The UBM color flow mapping in the sagittal view was diagnosed as pulmonary artery and majority of aorta connected with the RV, but no obvious flow from the PA and a possible subaortic VSD, which together indicated DORV with severe pulmonary stenosis.

Video 4E: EFIC movie displayed DORV with severe pulmonary stenosis and AVSD. There was also a hypoplastic branch pulmonary artery with PDA.

VIDEO 5

Video 5A: Vevo2100 color flow imaging in the sagittal view revealed hypoplastic aorta with reversal of aortic blood flow, indicating severe aortic stenosis. Note blood flow from the descending aorta into the ascending aorta, with only very small flow through the aortic valve.

Video 5B: Hypoplastic LV as seen by Vevo2100 2D imaging in the transverse view.

Video 5C: Quicktime movie of EFIC serial 2D image stack showed hypoplastic aorta with severe aortic stenosis, and hypoplastic left ventricle with hypoplastic mitral valve, which together comprises HLHS.